AD-A179 047 AN ANALYSIS OF SELECTED SATELLITE DATA OF THE AEGEAN AREA WITH THE SIARS SOFTWARE(U) SACLANT ASW RESEARCH CENTRE LA SPEZIA (ITALY) B WANNAMAKER NOV 86 1/1

UNCLASSIFIED SACLANTEN-SR-103 F/G 8/10 NL

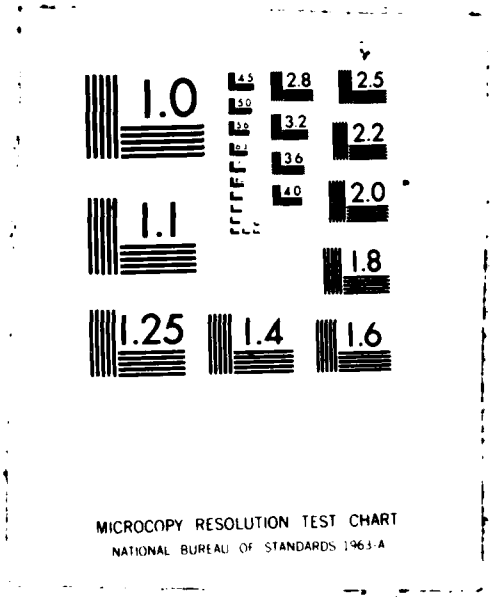
1.0
1.1
1.25
1.4
1.6
1.8
2.0
2.2
2.5
2.8
3.2
3.6
4.0
MICROCOPY RESOLUTION TEST CHART
NATIONAL BUREAU OF STANDARDS 1963-A

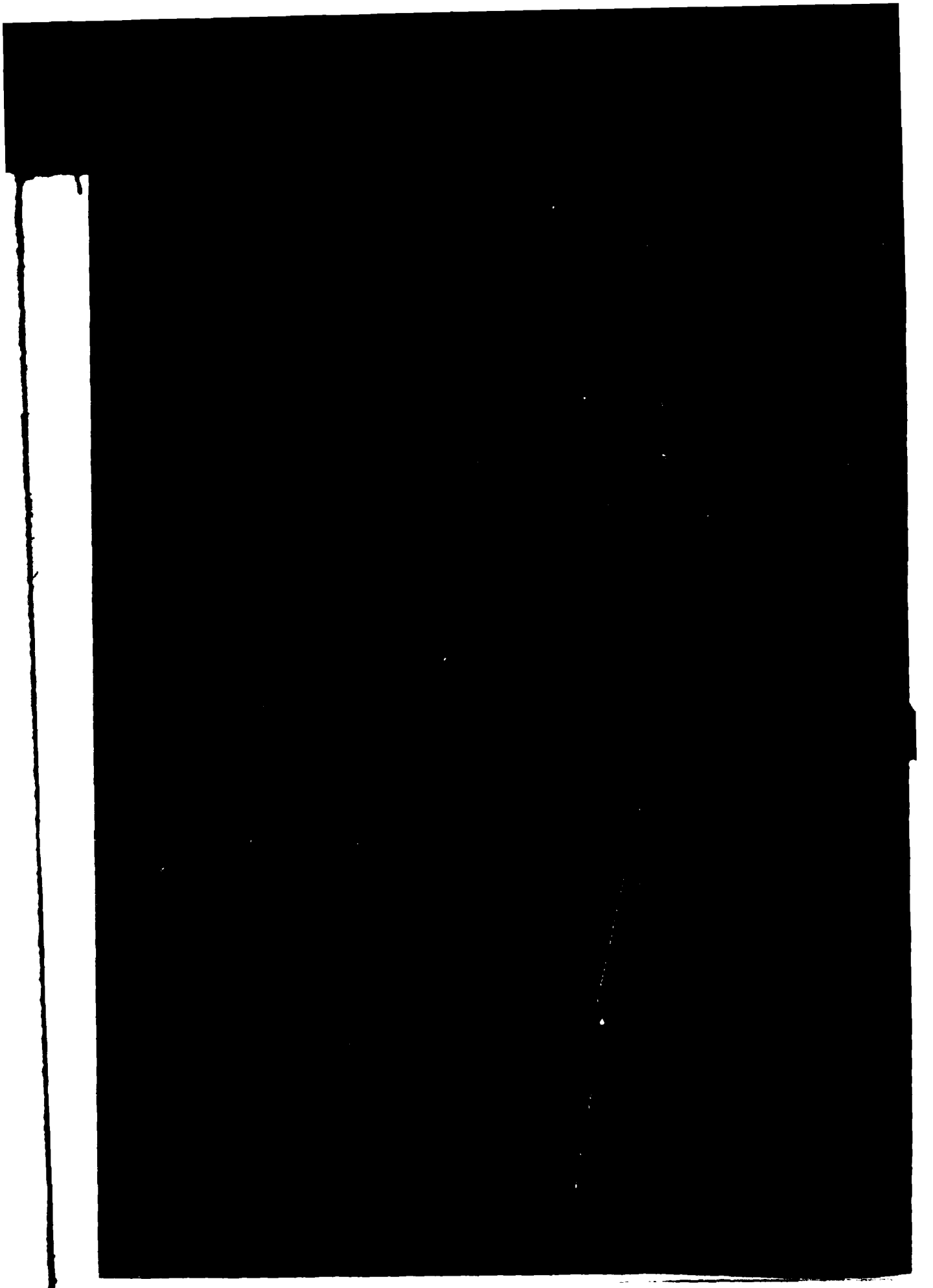

SACLANTCEN REPORT SR-103

NORTH ATLANTIC TREATY ORGANIZATION

SACLANT ASW Research Centre
Viale San Bartolomeo 400,
I-19026 San Bartolomeo (SP), Italy.

tel: national 0187 540111
international + 39 187 540111

telex: 271148 SACENT I

AN ANALYSIS OF SELECTED SATELLITE DATA OF THE AEGEAN AREA WITH THE STARS SOFTWARE

by

Brian Wannamaker

November 1986

This report has been prepared as part of Project 23.

APPROVED FOR DISTRIBUTION

Ralph R. Goodman

RALPH R. GOODMAN
Director

CONTENTS

Abstract

Data from selected orbits of the NOAA-7 meteorological satellite are used for an exploratory analysis of the surface variability in the area of the Aegean Sea using the STARS software system. The data suggest that a patch of cooler water (< 22°C in summer) in the northwest Aegean is due to mixing in the Dardanelles. Another cool patch in the Gulf of Corinth may be due to wind-induced upwelling and tidal-induced mixing. Excellent correlation is found between albedo (here a measure of surface roughness) and surface temperature, with low albedo associated with high temperature; the relative patterns are displaced spatially depending upon the topography of the adjacent shoreline.

1. Introduction

One of the reasons for the installation of a satellite receiving station at SACLANTCEN (Wannamaker, 1983) was to monitor the features visible in the imagery for indications of areas subject to variability and perhaps therefore deserving further study. This report deals with one such area.

During the summer of 1982 data from a number of satellite passes over the eastern Mediterranean were received in support of a research cruise. Certain surface temperature features beyond the limits of the cruise investigations were noted in the data, in particular a region of relatively cool water extended outward from the Dardenelles and another region of cool water existed in the Gulf of Corinth. It was decided to make a preliminary investigation of the area with material from the satellite data archive.

SACLANTCEN holds digital tapes of selected APT (Automatic Picture Transmission) data of NOAA-6 and NOAA-7 satellites dating from May 1982 and roughly 150 tapes of the HRPT (High Resolution Picture Transmission) data extending back to August 1979. APT and HRPT are separate simultaneous transmissions of data from the Advanced Very High Resolution Radiometer. The APT format is an analogue transmission of averaged data at two of the five channels of the instrument. Figure 1 of 17 October 1983 shows a typical image of the area in this format. SACLANTCEN digitizes these data at reception in order to analyse them quantitatively (Wannamaker, 1983). The HRPT format is a digital transmission of 5 channels of data, with a nominal ground resolution of 1 km.

2. Data

After a scan of the quick-look images of the archive, it was decided to concentrate on the NOAA-7 Orbit 5224. This crossed the equator on a northbound pass at 12:26:35 GMT on 28 June 1982 and was over the eastern Mediterranean at about 12:37 GMT.

The relevant part of the image was transferred to the STARS system and data from three channels were selected: Channel 2 in the near-infrared at ~0.85 μm, and Channels 4 and 5 in the thermal infrared (IR) at~11 and~12 μm. The data are stored on disk with 8 bits per picture element (pixel), and for the thermal IR channels this was done in such a way that full precision (10 bit) was retained in the temperature range from approximately 12°C to 28°C, with reduced resolution over the rest of the range from -30°C to +40°C (Wannamaker, 1983).

The near-infrared Channel 2 image confirmed that there was little cloud in this area. The coastlines were very distinct and the image from this channel was used to 'navigate' the data, which involves the interactive location in the image of known features on the earth surface (ground control points) in relation to their positions estimated by the computer program. The ground control points in this area are listed in Table 1 and were automatically retrieved from the master library (Wannamaker and Nacini, 1984; Wannamaker et al., 1986). The results of the navigation process are used to estimate the altitude and changing attitude of the spacecraft during the period of data acquisition, which subsequently allows the transformation of the images to standard map projections. In order to preserve the full satellite sensor resolution, two sets of images were generated in Standard Mercator projections: one centred at 39.5°N, 27°E and the other at 38°N, 23°E. The central latitude in each case was taken as the reference latitude where 1 pixel = 1 km^2. The two remapped images from the near-infrared channel are shown in Figs. 2a and 2b.

Each channel had been calibrated before the data were mapped and the two thermal IR channels were subsequently combined using the expression

$$T_S = 3.488\ (T_4) - 2.488\ (T_5) - 0.319,$$

where

T_S = absolute sea-surface temperature measurement corrected for the intervening atmosphere,

T_4 = brightness temperature value in Channel 4,

T_5 = corresponding value in Channel 5.

The resultant sea-surface temperature images are shown in Fig. 3.

The mapped images show a number of interesting features which are discussed after the general meteorological situation has been outlined.

3. Weather map

The synoptic situation shown in Fig. 4 indicates a low pressure area (< 1000 mb) over Lithuania extending a cold front southeasterly, and also westerly trailing over central Greece. Only a few cloud streaks are noted in the images, and they are aligned with the front. A secondary low (< 1005 mb) is reported on the chart centred over the N. Aegean, with winds of about 5 to 10 kn. There was scattered cumulus over the land. The line of cold front had moved about 37 km south-east since the midnight chart (approx. 0.9 m/sec).

4. Analysis of satellite images

The satellite data shows the coldest water in the area to be along the south coast of the Black Sea, where the surface temperature has an average value of 16.5°C, with an extreme value of 15.6°C at one point. A major river enters the Black Sea in this area, and the reported wind near the area is southerly, perhaps inducing upwelling. The cooler water of the Black Sea enters the Sea of Marmara. The surface outflow of the Dardanelles is cooler than the surface temperature in the Sea of Marmara and extends into a cool patch about 65 km long in the east-west direction and roughly 30 km wide. Generally the Aegean Sea has a mottled appearance typical of 'anomalous surface heating' under low wind conditions (Fett et al., 1977). The temperature is obviously higher on one side of the islands with localized cold patches also evident in both Figs. 3a and 3b. Another feature to note is the cooler water in the Gulf of Corinth. In the Ionian Sea cooler water indicative of upwelling along the islands and promontories of Greece is carried along in a southeasterly surface flow. Some of these features will now be discussed in more detail; Fig. 5 shows the locations of place names used in the text.

5. Dardanelles outflow

The relatively cool (< 22.5°C) patch of water covering an area of some 2200 km^2 lying to the south and east of the island of Limnos appears to emanate from the Dardanelles. The average temperature of the area is 21.84°C, σ= 0.54 K). This is significantly cooler than the surface of the western end of the Sea of Marmara (T = 25.10°C, σ = 0.39 K).

To further characterize the temperature in this area, three profiles were taken as shown in Fig. 6. The first profile (from the island of Ayios Evstratios to the cape of Ilyasbaba) cuts through the northern part of the pool, indicating rather ragged boundaries with multiple crossings of warmer water (Fig. 7).

The second profile (from the island of Limnos to Lesvos) indicates a sharp southern boundary about 34 km along this southeasterly line, with a temperature rise of 1.7 K over a few kilometres.

From the third profile, being nearly north-south at about 25.5°E, the extent of the patch is 38 km. Along both of the second and third profiles the coldest temperature encountered was 20.1°C. A similarly placed profile was taken from the APT image of 3 weeks later, 21 July 1982. At this time, with just one thermal IR channel available, the data were not corrected for the effect of the atmosphere. This profile, included in Fig. 7, indicated a sharp drop of 4°C over 3 km at the northern boundary of the patch and a gradual warming to the south. The land-sea boundary of the west coast of Turkey was not marked by a sharp temperature contrast, possibly due to radiation cooling of the land to near sea temperatures or due to coastal fog. Without the second IR channel the possibility cannot be ignored that the profile data may include measurements from a fog layer.

An APT image for July 30, 1982 showed the cool patch in the Dardanelles Outflow to be a different shape, and the temperature drop was only 1 K. However, since this area lay near the edge of the image, where the effect of the atmosphere is greatest, this value may not be reliable. Nevertheless these data imply that the cool patch is not a static feature.

A profile along the Dardanelles itself (Fig. 8) and into the Sea of Marmara implies that the surface cooling occurs at the point where the channel changes direction sharply (point A) and near the entrance to the Strait (point B). Some profiles across the Strait indicate cooler water along the southern shore but not all of the profiles confirm this observation and the distance is too short compared to the resolution of the satellite sensor for it to be accepted without further evidence. One hypothesis is that the funneling and turbulent mixing in the shallow Dardanelles incorporates water from below the thermocline into the surface layers. Data taken by Defant (Defant, 1961; Officer, 1976) in autumn (October), with the wind in the direction of the surface current (40 cm/s), indicate the pycnocline rising smoothly 19 m from the Sea of Marmara to the Aegean.

6. Inter-island upwelling

An interesting structure was apparent along the line of the Greek Islands of Euboea, Andros, Tinos and Mikonos in both the near-IR and IR imagery. Profiles were taken along the line shown in Fig. 9 and are shown in Fig. 10. This is an afternoon image with the sun's spe-

cular position well to the west. Hence the sunlight would be reflected away from the satellite sensor if the sea were calm. In a wind-roughened sea, however, some of the wave facets would be at the proper angle to reflect light into the sensor. Hence a higher radiance value from the sea surface represents a rougher surface and in turn higher wind speed.

In the straits between the islands a higher wind speed caused by funnelling of the wind has created a rougher surface and also the upwelling of cooler subsurface water. Also shown in Fig. 10 is a schematic of the topography of the islands along a line perpendicular to the estimated wind direction. These values were taken from a nautical chart with contour intervals every 1000 ft (305 m). Unless expressly given on this chart, all values between contour intervals were assigned to the midpoint value.

Consideration of the profiles shows, as expected for alongshore flow, that the point of upwelling and the minimum temperature are against the coast, to the left of the maximum wind looking downwind. In the lee of the islands there is virtually no wind mixing and the incoming solar radiation is trapped in the surface layer, which becomes 'anomalously hot'. Where there is a break in the topography, the wind blowing offshore can sweep away surface water and cause upwelling and vertical mixing. Thus at these locations areas of coolest surface temperature are aligned with the highest radiances or windspeeds. Although there are other factors involved, such as the shapes of the islands, surface currents and smaller scale topography, there is an excellent correlation between high topography, low winds and high temperatures, and cooler temperatures where the windspeed was higher.

7. Gulf of Corinth

An area of about 730 km^2 of the Gulf of Corinth was covered with water with a temperature of less than 22°C; the average was 20.84°C (σ = 0.69 K) and the minimum was 19.82°C. Winds at a meteorological station on the north-west coast of Greece were reported as westerly at 15 kn. This is supported by the evident upwelling on the south-western coasts of the islands and Peloponnese. This wind, funnelled into the Gulf of Corinth, could be expected to induce mixing and upwelling of cooler water in the Gulf. Nautical charts show tidal currents in the 2-km-wide entrance to be between 1 and 2 kn. The wider entrance to the Gulf is much shallower, 60 m, and may be warm to the bottom. The Gulf itself extends to depths of 934 m (Heezen et al., 1966). Upwelling also occurred in the Gulf of Saronikas across a narrow peninsula from the city of Corinth. At this time of day in summer, the Gulf of Athens is usually dominated by onshore winds which would block the northwesterlies from inducing upwelling in this area. Figure 11 shows a temperature profile through the area and the position of the profile line.

8. Island heat shadows

In the thermal IR images it is apparent that the sea temperature on one side of most of the islands is significantly higher than on the other. These warm patches extend some distance away from the islands, usually decreasing in width with distance. Two possible reasons for this are that the islands are blocking the wind flow and preventing wind-mixing as discussed above, or that moist air passing over the islands has become drier and/or warmer and is thus decreasing the attenuation of the signal reaching the spacecraft. The latter seems unlikely in this case because there is no evidence of precipitation or cloudiness on the upwind sides of the islands. In either case these 'heat shadows' lie on the leeward side of the islands and extend downwind. Figure 12 shows a schematic map of the area with arrows indicating the estimated wind direction as the axis of the warmer features. These are consistent with the synoptic situation depicted in the weather map of Fig. 4 and local topography. These patterns are a useful indicator of wind flow. A curious exception to this is a warm patch (> 27°C) of the south coast of the island of Lesvos. This is on the expected windward side of the island and lies over a depression in the sea floor. The depth of this dip is more than 300 fathoms (550 m), whereas the general depth in the area is between 100 and 200 fathoms (180 to 365 m).

9. IR channel difference

Shown in Fig. 13 is an image obtained by subtracting Channel 5 from Channel 4 (and adding a bias of 20 K). This should give some measure of the amount of water vapour in the atmosphere. Clouds show up clearly in white. Atmospheric internal waves with a wavelength of about 7 km are evident over the north-western Greek islands, apparently caused by the wind flowing over the island of Cephalonia. Also evident is the boundary between cooler water upwelled along the southwest coast of Greece and the Ionian Sea water, suggesting a possible change in atmospheric water vapour at the boundary — since the air-sea temperature difference affects the stability and humidity of the overlying layer (Sweet et al., 1980). The cool water patch in the Gulf of Corinth (discussed above) is also evident, possibly for the same reasons. This indicates the value of multiple IR channels, since by proper combination these atmospheric effects can be largely removed from the single-channel estimates of temperature.

Another point to be noted is the white boundaries of the eastern edge of islands and the black boundaries of the western edges. This is the result of a slight misregistration between the fields of view of Channel 4 and Channel 5, whereby the latter senses a boundary first. This misregistration is not sufficient to create noticeable noise at oceanic fronts.

10. Conclusions

The APT data have indicated an area of surface variability in the Mediterranean Sea and the APT data archive has been used to do a quick preliminary survey of an area using one HRPT image and a few APT images. Thus the APT receiving system and data archive has successfully met one of its design objectives.

The area surveyed was the Aegean and Gulf of Corinth, and hypotheses have been presented for the causes of features apparent in the data:

Observation 1

A cool patch of water in the north Aegean covering some 2200 km^2 has its source in the Dardanelles. It is suggested that it results from mixing in that Strait between the surface and cooler underlying water caused by the venturi effect of the narrow Strait and the right angle bend in its course. APT data, some of which was not discussed in detail in this report, indicated that this patch does vary in extent under different wind conditions.

Observation 2

Under wind speeds reported as around 10 kn (5 m/s), upwelling occurred at particular points off many of the Aegean islands. Along the island chain of Euboea, Andros, Tinos and Mikanos, profiles of temperature and near-IR albedo indicated that the albedo can be a reliable indicator of upwelling. Between the islands the channeled wind was alongshore and the coldest temperatures (about 2 K below average) were found to the left of the strongest wind (highest albedo) looking downwind. Where the wind blowing over an island induced surface temperature cooling by mixing or upwelling, the coldest temperature was aligned with the highest albedo.

Under the conditions encountered on the day of the HRPT image, the islands blocked the wind creating heat shadows behind them. By taking the estimated wind direction as the axis of these patterns, a picture consistent with the meteorological situation was obtained. In the absence of convential data this technique could be used to predict the direction (and possibly the strength) of low level winds.

Observation 3

An area of cooler water exists in the Gulf of Corinth in the deep water east of the sill, which is at the narrowest point of the Gulf. It is suggested that it is due to wind-induced mixing aided by strong tidal currents.

Observation 4

Some of the surface features in the surface temperature imagery were also evident in the image obtained by taking the difference between Channels 4 and 5, and might be due to change in the near-surface atmosphere resulting from a change in air-sea temperature. This was not as evident in the easterly portion of the data and it is suggested that this is as result of the different overlying air mass to the east of the cold front crossing Greece, although this would place the front some 30 to 50 km southwest of its location on the synoptic chart.

This was a preliminary analysis based on a few satellite images. Obviously for a full understanding of the phenomena, measurements from ships are required. If this were to be done it is suggested that first of all there should be further analysis of the satellite imagery in the archive; the objective would be to determine the temporal changes in the surface expressions of the features and their relation to surface winds and other factors.

References

DEFANT, A, Physical Oceanography, volume 1. New York, NY, Pergamon, 1961.

FETT, R.W., and MITCHELL, W.F. Navy tactical applications guide, volume 1: Techniques and applications of image analysis. Monterey, CA, Naval Environmental Prediction Research Facility, 1977. [AD B 024 969]

HEEZEN, B.C., EWING, M. and JOHNSON, G.L. The Gulf of Corinth floor, Deep-Sea Research, 13, 1966: 381-411.

OFFICER, C.B., Physical Oceanography of Estuaries and Associated Coastal Waters. New York, NY, Wiley, 1976.

SWEET, W., FETT, R.W., KERLING, J. and LA VIOLETTE, P. Air-sea interaction effects in the lower troposphere across the north wall of the Gulf Stream, Monthly Weather Review 109, 1981: 1042-1052.

WANNAMAKER, B. 1983, A system for receiving and analysing meteorological satellite data at small meteorological oceanographic centres or aboard ship, SACLANTCEN SR-74. La Spezia, Italy, SACLANT ASW Research Centre. [AD A 137 215]

WANNAMAKER, B., and NACINI, E. 1984, A directory of European, Middle Eastern, and N. African coastal ground control points for mapping satellite images, SACLANTCEN SM-170. La Spezia, Italy, SACLANT ASW Research Centre. [AD A 142 019]

WANNAMAKER, B., NACINI E. and MINNETT, P.J. 1986, A directory of ground control points for mapping satellite images over the Northeastern Atlantic Ocean and adjacent seas, SACLANTCEN SR-93. La Spezia, Italy, SACLANT ASW Research Centre.

FIGURES AND TABLES

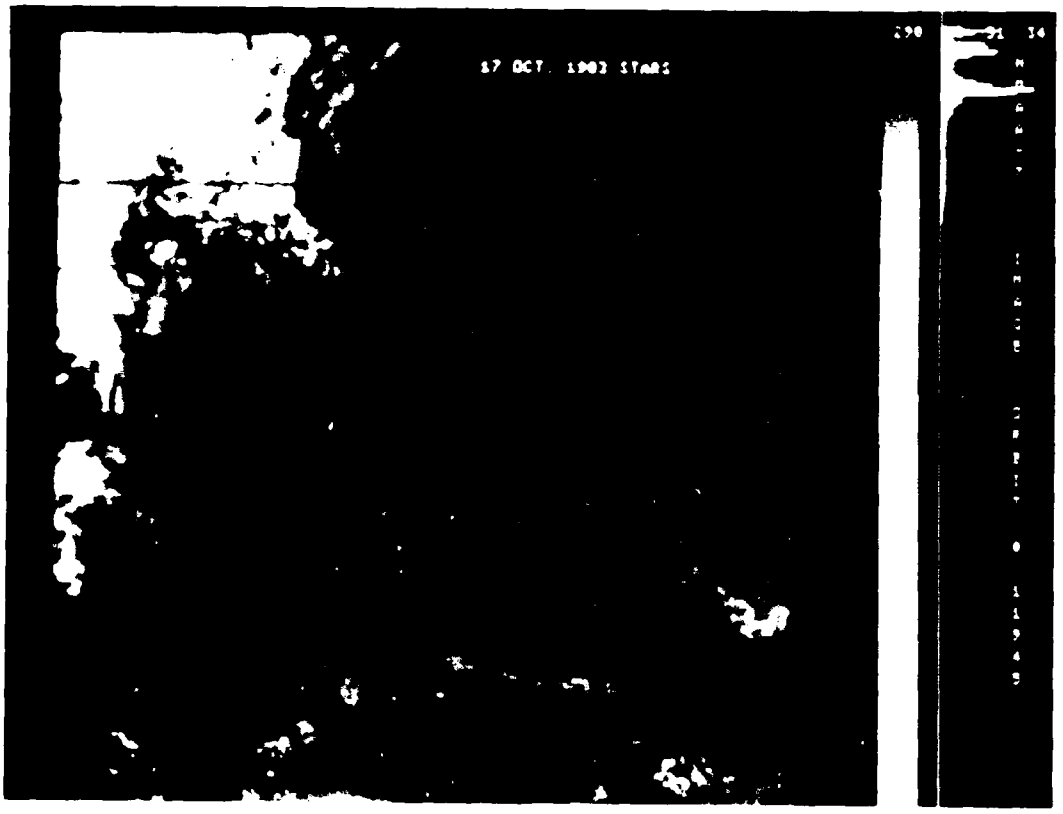

Fig. 1 An APT (Automatic Picture Transmission) near-IR image of the eastern Mediterranean area. Nominal resolution is 4 km per picture element.

Table 1

Ground Control Points in the raw image; their true geodetic positions and estimated positions in the image on the computer disc.

N	DESCRIPTION	LATITUDE	LONGITUDE	ALTITUDE
1	ISTANBUL	41.000	28.983	36.0
2	C.S.MARIA DI LEUCA 216	39.797	18.369	53.5
3	N.OTHONI A. KASTRI 242	39.864	19.422	98.0
4	N.KERKIRA A. ARILLA 243	39.708	19.654	25.0
5	N. " A.LEVKIMMIS 244	39.462	20.074	5.0
6	VRAKHOI LAGOUDHIA 245	39.418	19.904	15.0
7	N.PAXOI AKRA LAKKA 246	39.242	20.125	55.0
8	AKRA MITIKAS 247	38.997	20.701	6.0
9	N.LEVKAS YIRAPETRA 248	38.850	20.721	9.0
10	NISIS SESOULA 249	38.700	20.538	33.0
11	N.LEVKAS DHOUKATON 250	38.566	20.542	60.0
12	N.KEFA. A.DHIKHALIA 251	38.283	20.676	13.0
13	" A.YEROGOMBOS 252	38.182	20.342	34.0
14	N.VARDHIANOI 253	38.134	20.429	4.0
15	N.KEFA.A. KATELIOS 254	38.062	20.746	75.0
16	N.ZAKINTHOS SKINARI 255	37.933	20.700	57.0
17	" A.KRIONERI 256	37.807	20.903	13.0
18	" A.KERI 257	37.653	20.818	182.5
19	AKRA KATAKOLON 258	37.640	21.317	36.0
20	N.SAP.DHIO ADHELFIA 259	36.742	21.697	102.0
21	AKRA LIVADHIES 260	36.799	21.967	10.0
22	AKRA KITRIES 261	36.916	22.122	20.0
23	AKRA TAINARON 262	36.387	22.483	25.0
24	AKRA MALEAS 263	36.450	23.200	0.0
25	AKRA ZOVOLLO 264	36.430	23.130	8.0
26	N ANDI A APLOITARES 265	35.825	23.324	28.0
27	SKIROS AKRA LITHARI 219	38.783	24.683	84.0
28	AKRA PSEVDHOKAVOS 220	39.950	24.000	35.0
29	AKRA AKRATHOS 221	40.133	24.400	37.0
30	ILYASBABA BURNU 222	40.050	26.183	25.0
31	BABA BURNU 223	39.483	26.067	22.0

Table 2

The results of the navigation process, giving the error between the true position as estimated by the operator and that determined after a statistical best-fit of the satellite motion.

GCP ESTIMATION ERRORS AND UPDATED POSITION:

GCP	DESCRIPTOR	LONGITUDE	LATITUDE	RESOLUTION	ERROR(METERS)	ERROR(PIXELS)
4	N KERKIRA A ARILLA 243	19.6118	39.6996	1005.59	3739.82	3.72
7	N PAXOI AKRA LAKKA 246	20.0897	39.2371	982.65	3096.06	3.15
12	N KEFA. A DHIKHALIA 251	20.6401	38.2642	970.67	3771.41	3.89
19	AKRA KATAKOLON 258	21.2923	37.6305	941.34	2419.00	2.57
25	AKRA ZOVOLLO 264	23.1326	36.4266	861.17	440.01	.51
27	SKIROS AKRA LITHARI 219	24.6948	38.7720	814.65	1599.15	1.96
30	ILYASBABA BURNU 222	26.1837	40.0498	856.43	65.94	.08
31	BABA BURNU 223	26.0877	39.4785	845.30	1846.61	2.18

NUMBER OF GCPS = 8 RMS ERROR IN METERS AND PIXELS = 2495 2993 2.6065

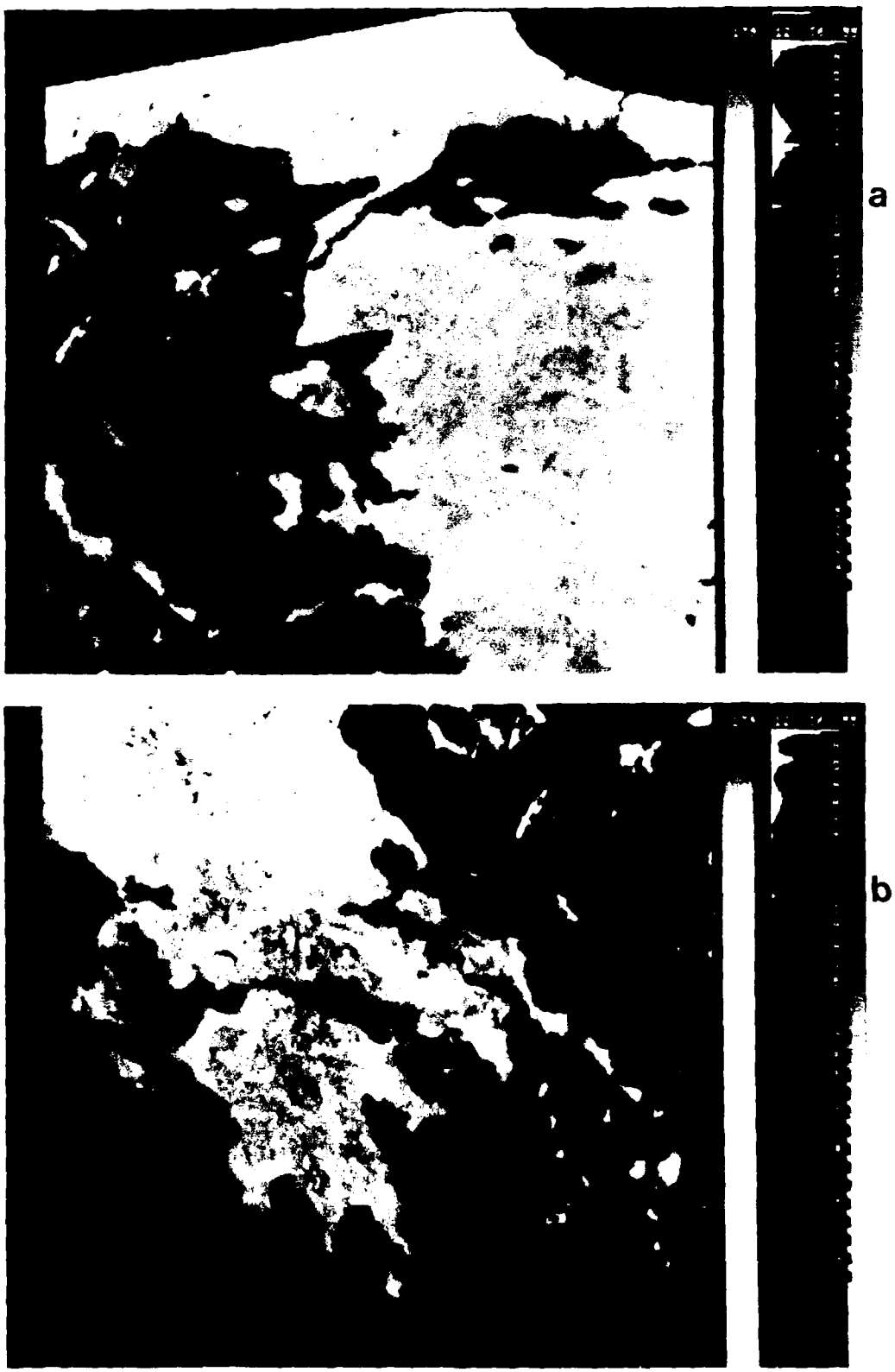

Fig. 2 The images mapped to a Mercator Projection
a) centred at 39.5°N, 27°E
b) centred at 38°N, 23°E

a

b

Fig.3a-b The sea-surface temperature images corresponding to Fig. 2.

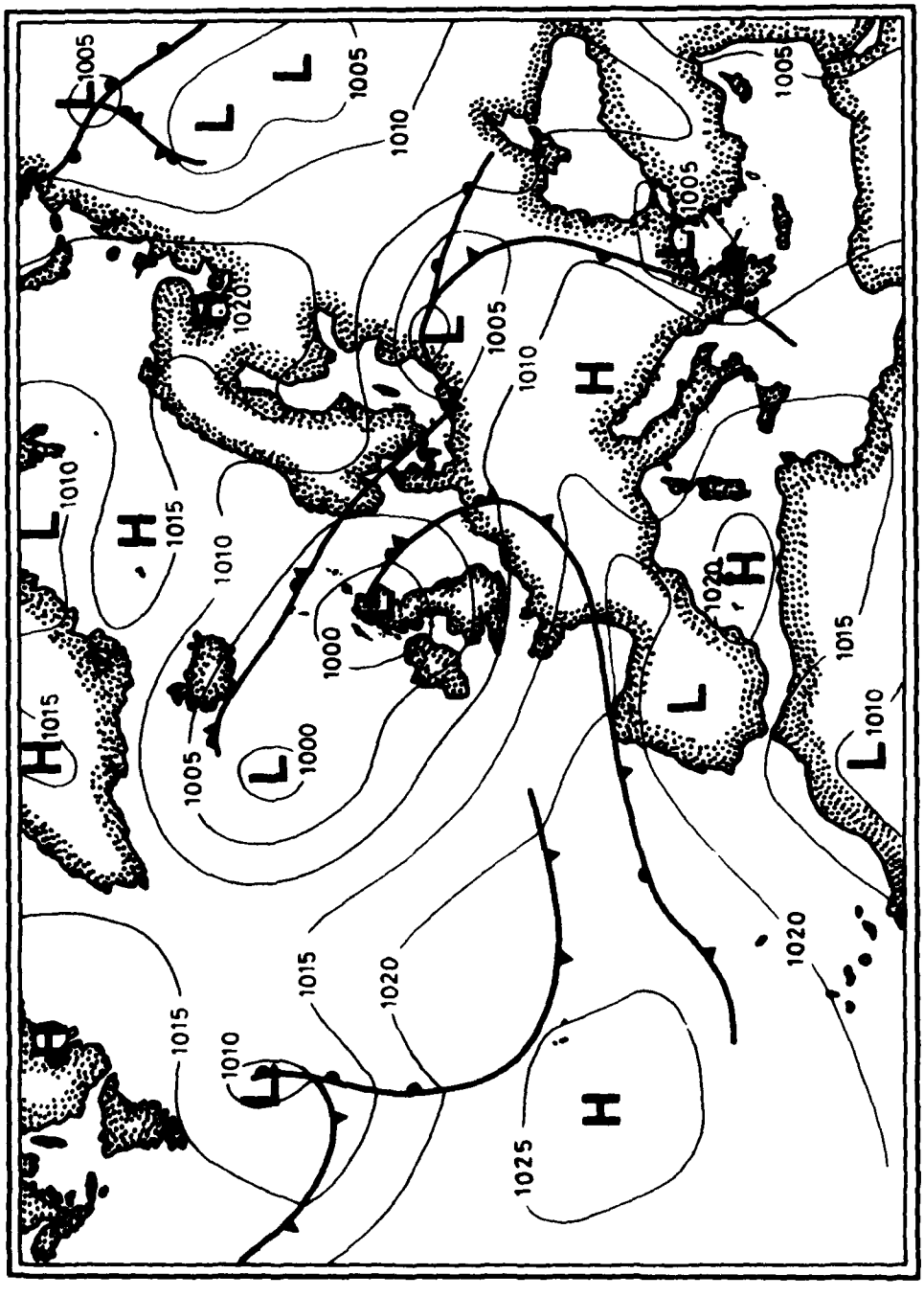

Fig. 4 Synoptic weather chart for 12 GMT 28 June 1982 (after European Meteorological Bulletin)

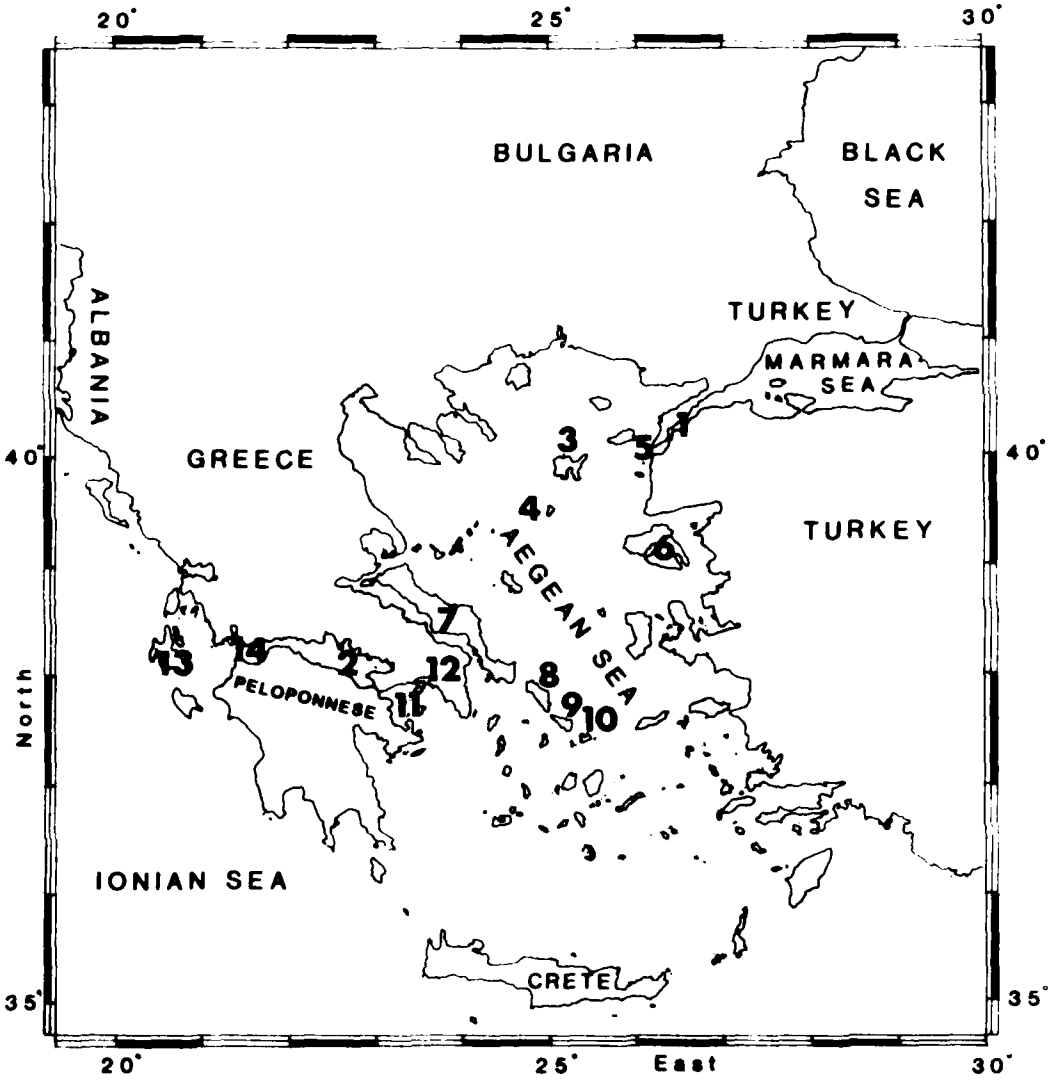

1. Dardanelles
2. Gulf of Corinth
3. Limnos I.
4. Ayios Evstratios I.
5. Ilyasbaba Cape
6. Lesvos I.
7. Euboea I.
8. Andros I.
9. Tinos I.
10. Mikonos I.
11. Gulf of Saronikos
12. Athens
13. Cephalonia I.
14. Gulf of Patra

Fig. 5 A chart showing the places named in the text.

Fig. 6 Positions of the three profiles through the Dardanelles outflow.

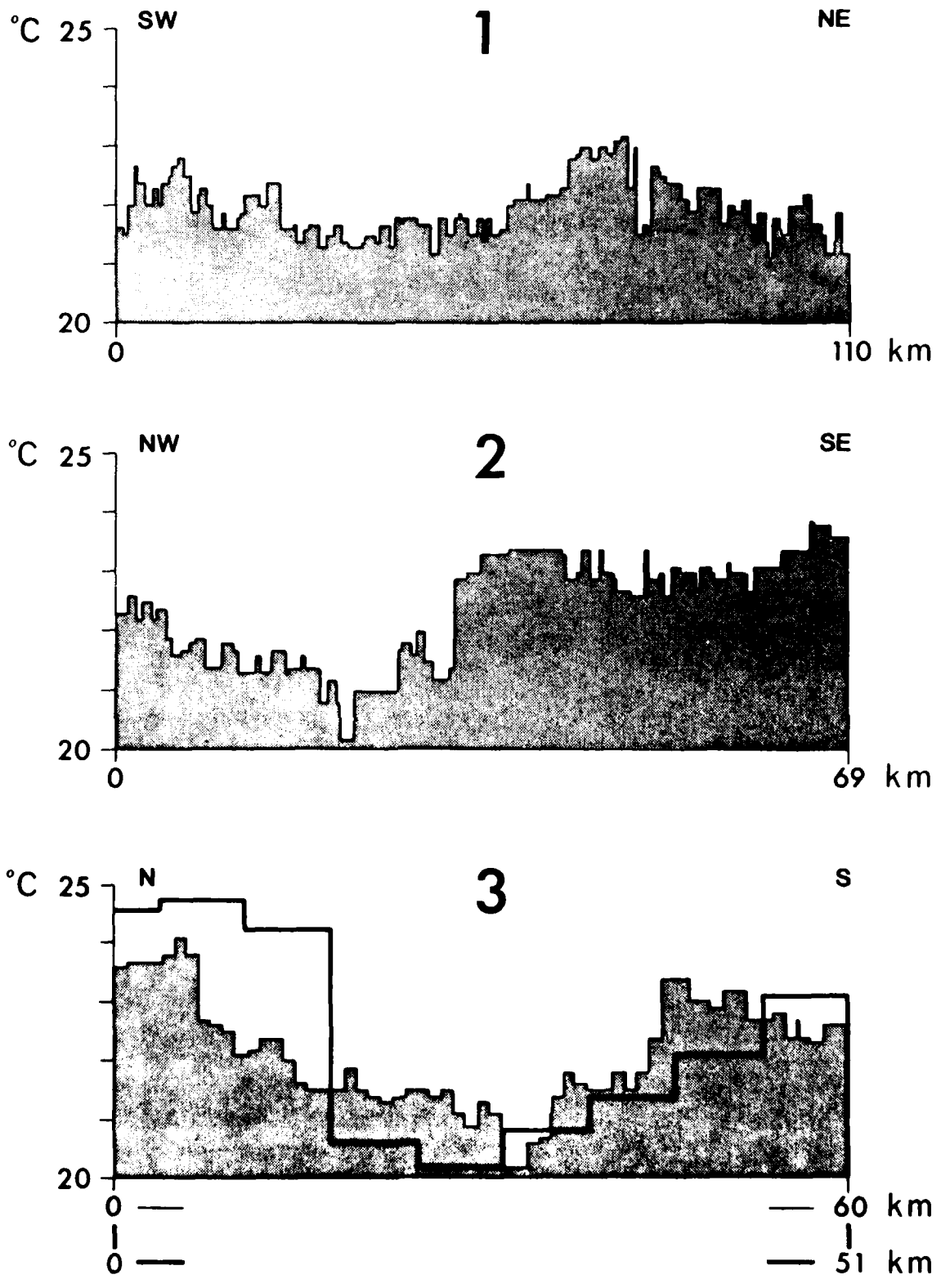

Fig. 7 The temperature profiles through the Dardanelles outflow as discussed in the text.

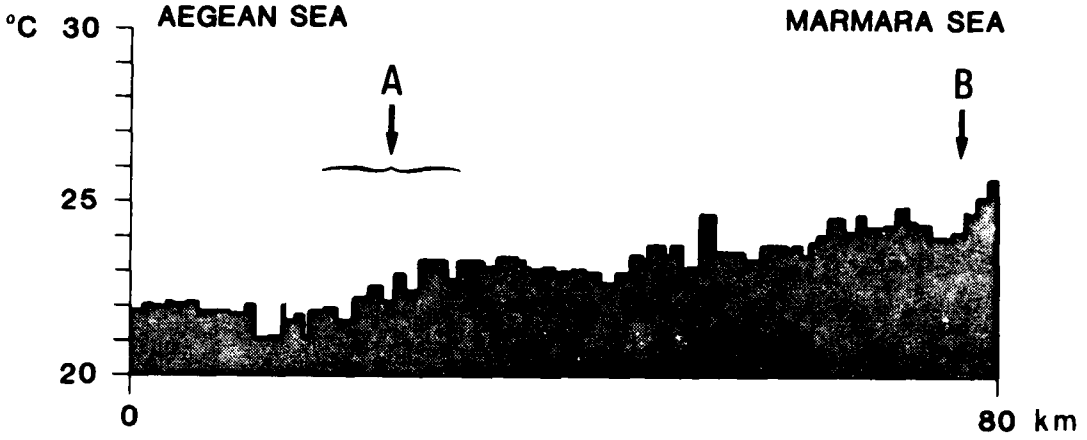

Fig. 8 A temperature profile fron the Aegean to the Sea of Marmara along the course of the Dardanelles, indicating that most of the temperature drop occurs at two locations.

Fig. 9 Positions of the temperature and albedo profiles along the Greek islands, marked on an image of thermal IR data (Channel 4 at 11 μm).

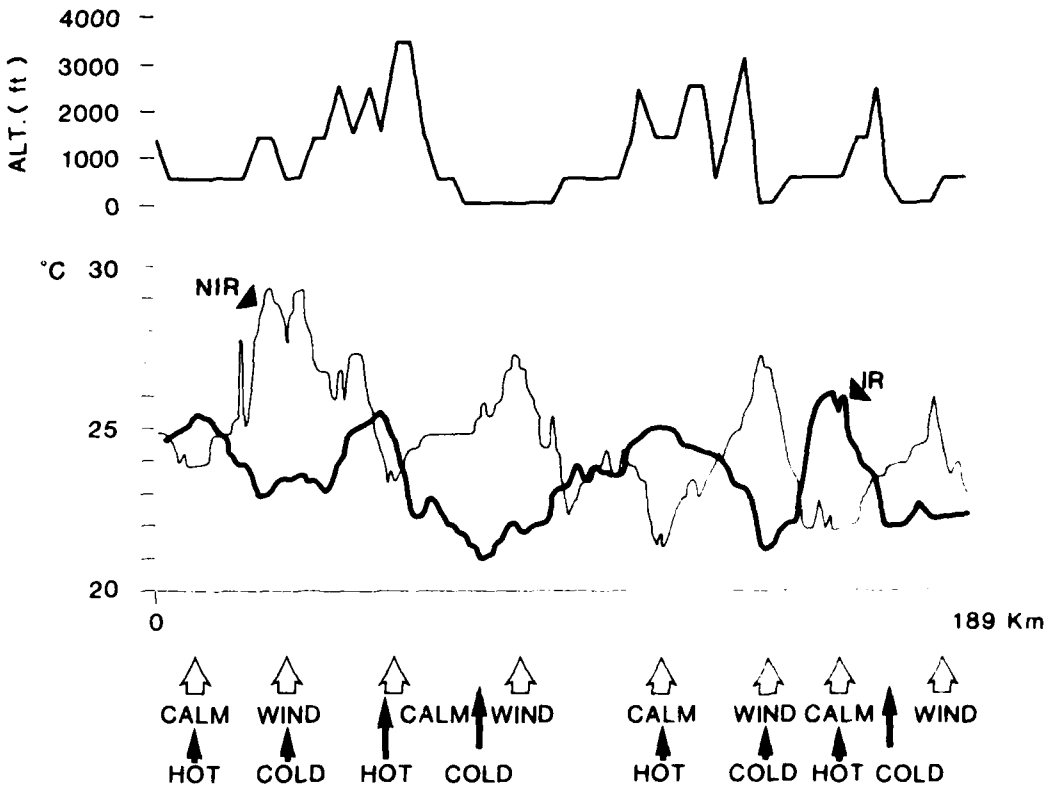

Fig. 10 Temperature and near-IR albedo along the line shown in Fig. 9. Also shown above is a schematic of the upwind topography of the islands upwind of the profile. The albedo can be taken as a measure of the surface wind speed (see text).

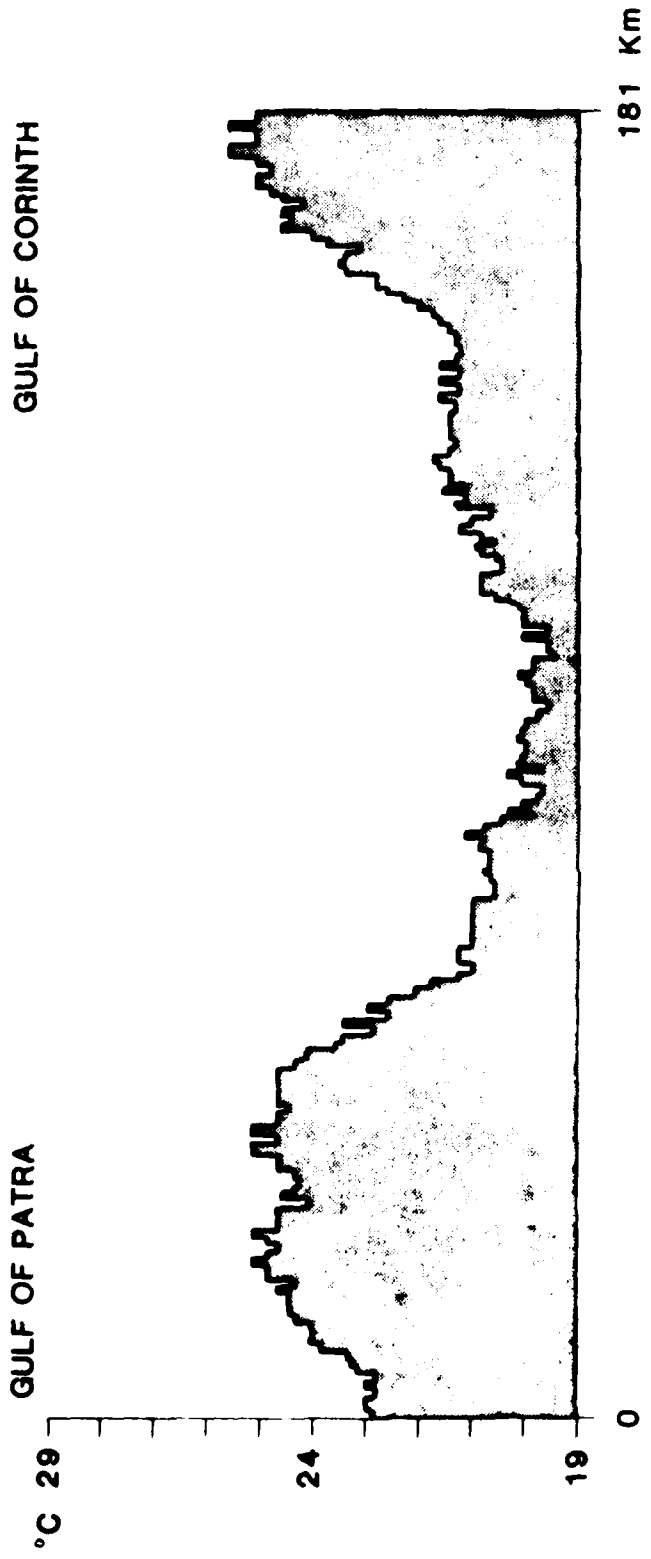

Fig. 11 a) Temperature profile through the Gulf of Corinth

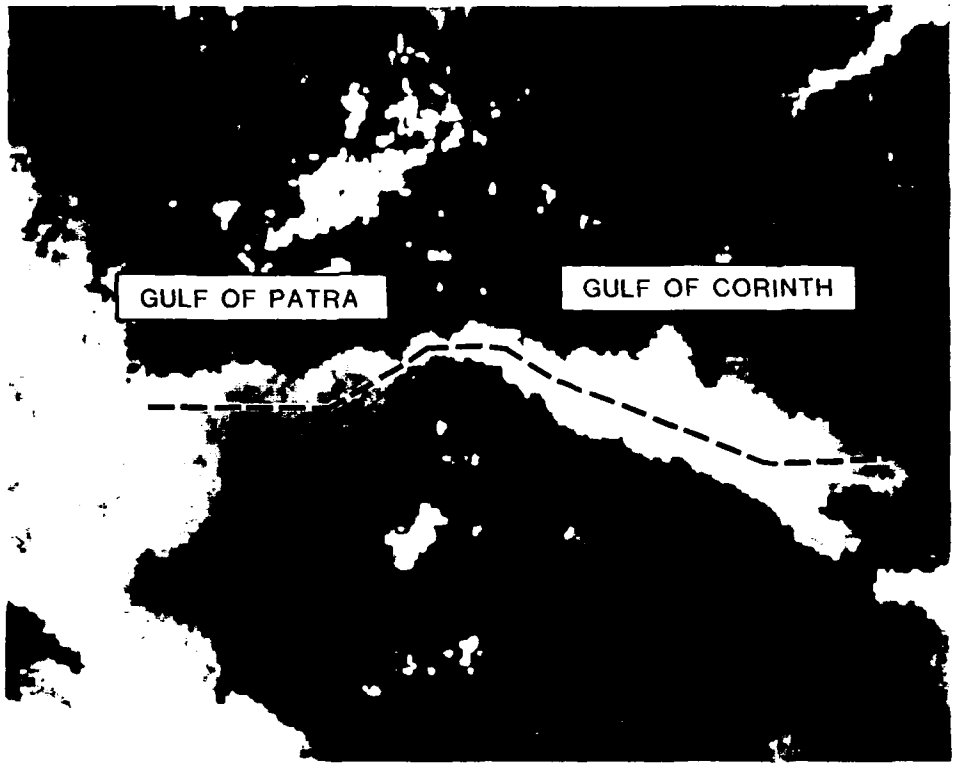

Fig. 11 b) Position of the profile in Fig. 11a)

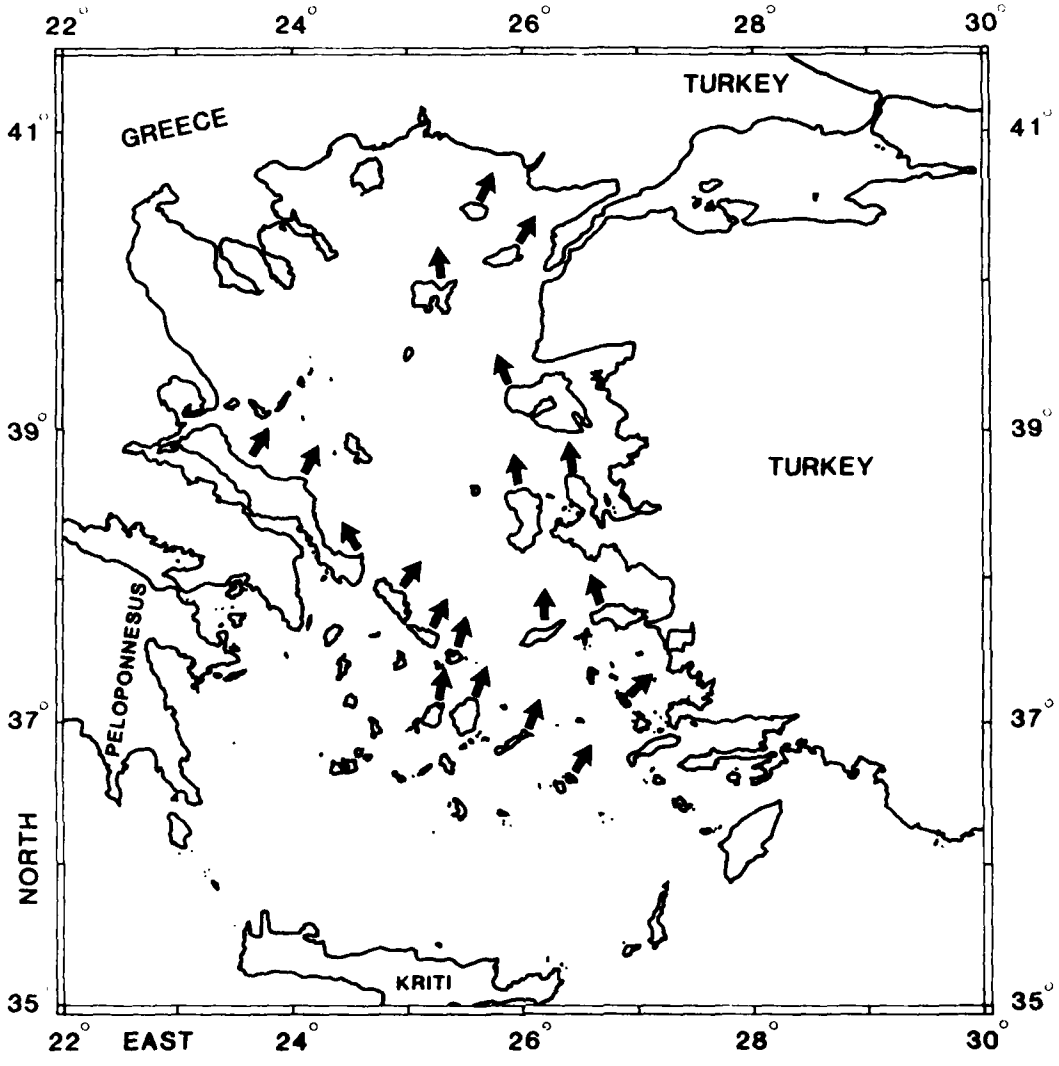

Fig. 12 Map of the area with estimated wind directions shown at selected sites based on the orientation of the heat shadows; c.f. the meteorological chart of Fig. 4.

Fig. 13 Image depicting the algebraic difference between the two IR images.

Keywords

AEGEAN
ALBEDO
DARDANELLES OUTFLOW
GULF OF CORINTH
HEAT SHADOWS
IONIAN SEA
MIXING
NOAA-7
REMOTE SENSING
SURFACE ROUGHNESS
SURFACE TEMPERATURE
SURFACE VARIABILITY
UPWELLING

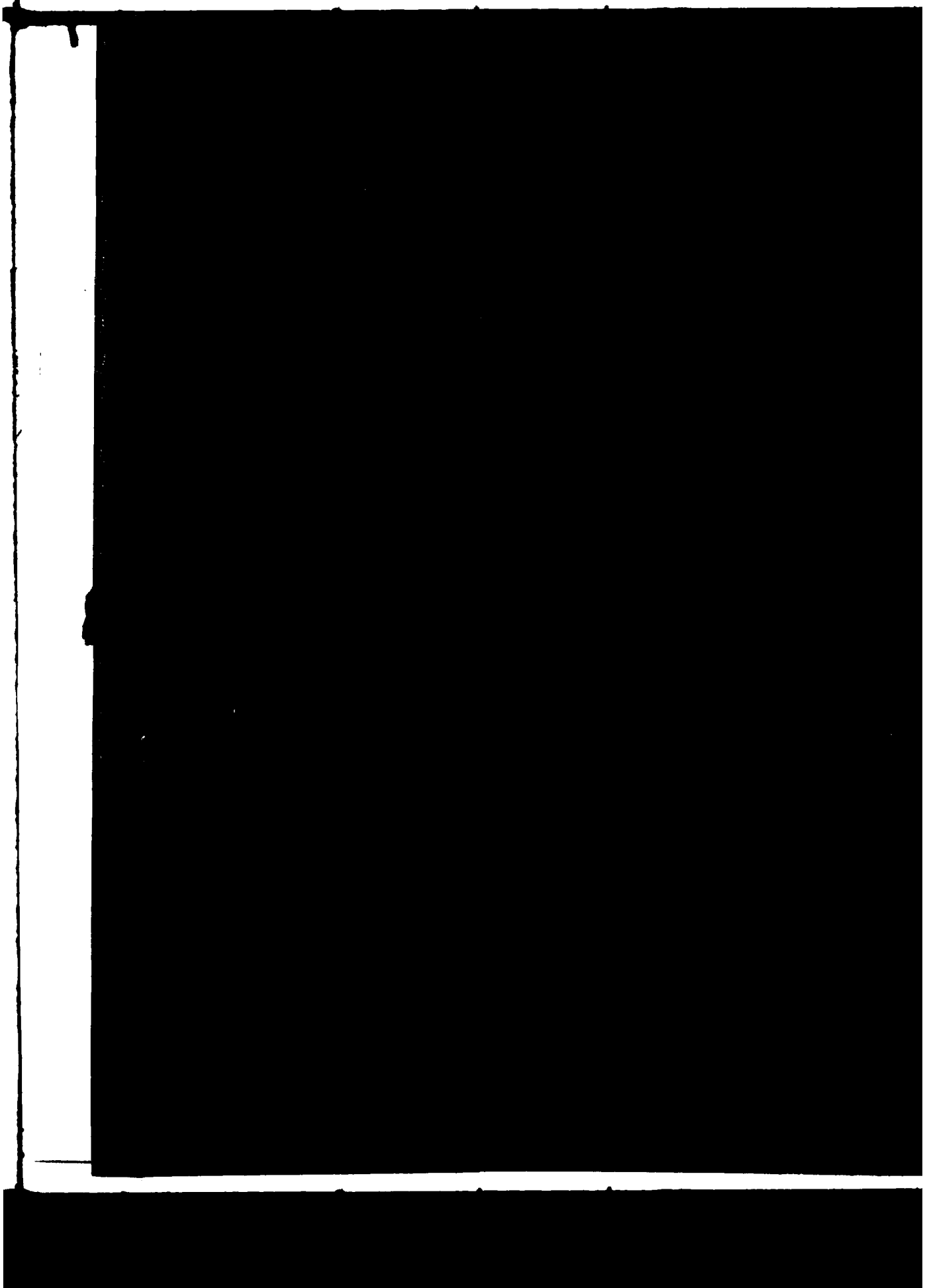


DAT
FILM